JOURNAL OF GEOPHYSICAL RESEARCH, VOL. 102, NO. B2, PAGES 2731-2749, FEBRUARY 10, 1997

Internal thermal boundary layer stability in phase transition modulated convection

Samuel Butler and W. R. Peltier

Department of Physics, University of Toronto, Toronto, Ontario, Canada

Abstract. The stability of a horizontal thermal boundary layer embedded within a very viscous fluid is investigated using the formalism of linear stability analysis. Thin thermal boundary layers in deep fluid regions and in the absence of phase transition and dynamical effects are thereby shown to be unstable at extremely long wavelengths. The stability of the internal thermal boundary layer which may exist at 660 km depth in the Earth's mantle as a consequence of the dynamical influence of the endothermic phase transition from γ spinel to a mixture of perovskite and magnesiowüstite, recently discussed in some detail by *Solheim and Peltier* [1994a], is investigated in order to better understand the "avalanche effect" observed in this and similar nonlinear, time dependent simulations of the mantle convection process. It is demonstrated that if the stability problem is treated as purely thermal, then the boundary layer is predicted to be extremely unstable and the presence of the 660-km endothermic phase transition at middepth within the boundary layer is further destabilizing. When the kinematic effect of flow convergence onto the boundary layer and phase transition region is active, however, it is shown that the layer may be strongly stabilized. In the regime of physically realistic velocity convergence, the critical Rayleigh number is predicted to lie in the range suggested by the numerical simulations of *Solheim and Peltier* [1994a]. A threshold value of the magnitude of the Clapeyron slope of the endothermic phase transition for a given velocity convergence is also shown to exist, beyond which the fastest-growing mode of instability changes from avalanche type to layered type.

Introduction

Although it is now well established that a thermally induced convective circulation exists in the Earth's mantle, there remain many unanswered questions as to its detailed physical characteristics. Foremost among these is the issue as to whether the circulation is "whole mantle" in style or whether a two-layer pattern exists that could be enforced by the endothermic spinel to post-spinel phase transition at 660 km depth (or perhaps by a chemical discontinuity). A number of nonlinear simulations have recently been described [e.g., *Machetel and Weber*, 1991; *Peltier and Solheim*, 1992; *Tackley et al.*, 1993; *Honda et al.*, 1993; *Solheim and Peltier*, 1994a, b; *Tackley et al.*, 1994; *Peltier*, 1996], which suggest that convection might, in fact, be layered by the influence of the phase transition alone. These layered states are intermittent, however, with avalanches consisting of cold downwellings breaking through the 660-km phase transition and causing episodes of brief but intense mixing to take place between the upper mantle and transition zone and lower mantle regions. It has also been suggested [*Peltier et al.*, 1996] that this source of intermittency of the circulation may be important to understanding the supercontinent cycle.

The question as to the criterion that must be satisfied for an avalanche to occur has come to be seen as important. *Tackley* [1995] has usefully studied this problem in the case of a single local upwelling or downwelling interacting with an endothermic phase boundary, while *Davies* [1995] has employed a parameterized convection model of the kind introduced by *Sharpe and Peltier* [1979] to investigate possible behaviors of time dependent phase change modulated convection. In the investigation to be reported herein, we will address the circumstance in which "ponding" at the phase boundary is pervasive and an internal boundary layer is established in the azimuthally averaged temperature field. Motivation for this analysis is provided by Figure 1, which is reproduced from *Solheim and Peltier* [1994a]. The diagnostic analysis of the axisymmetric spherical flow presented in this figure was performed on a statistically stationary simulation of convection heated from below at an Earth-like Rayleigh number of 10^7. The analysis demonstrates that if a local Rayleigh number is defined for the internal thermal boundary layer that develops at 660 km depth during the layered phase, Ra_{660}, then this Rayleigh number reaches a peak just prior to the occurrence of a typical avalanche (indicated by the peak in

Paper number 96JB03173.
0148-0227/97/96JB-03173$09.00

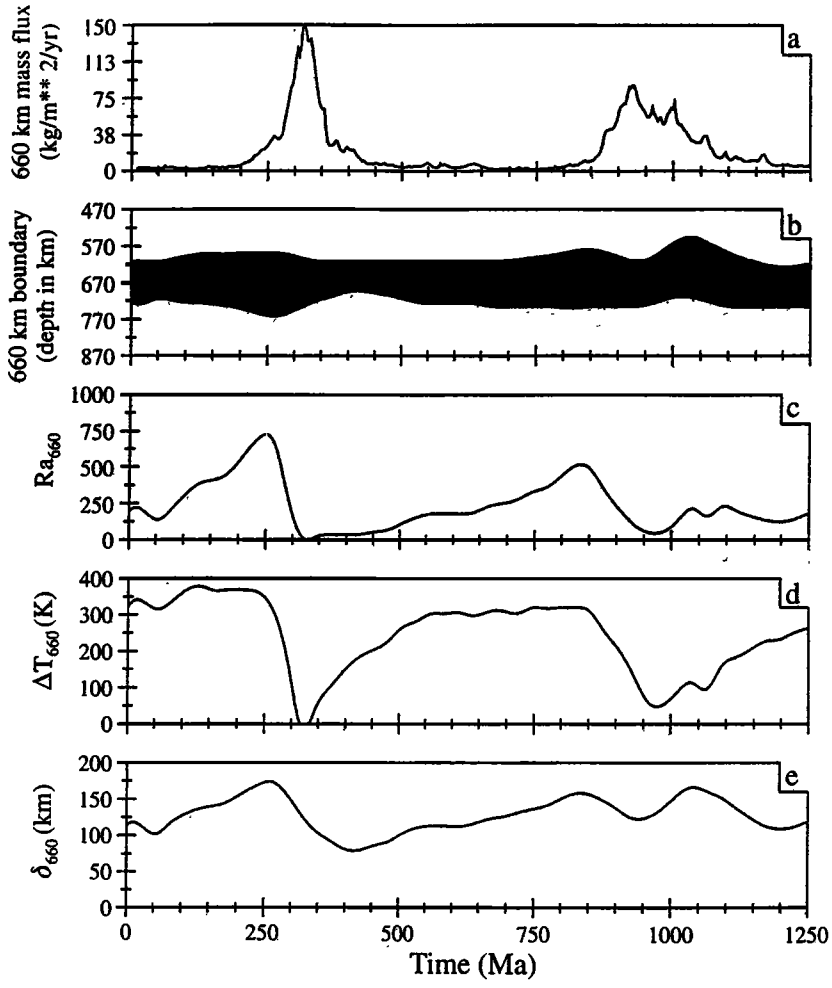

Figure 1. From *Solheim and Peltier* [1994a], illustrating the high mass flux events (avalanches) that occur across the 660-km phase transition following maxima in the boundary layer Rayleigh number, (a) mass flux, (b) boundary, (c) Rayleigh number, (d) temperature change, and (e) boundary layer thickness. The system Rayleigh number $Ra = 10^7$, the 660-km phase transition has a Clapeyron slope -2.8 MPa/K, and the convective circulation is heated entirely from below. The boundary layer Rayleigh number is defined as $Ra_{660} = (g\alpha\Delta T_{660}\delta_{660}^3)/(\kappa\nu)$, in which ΔT_{660} and δ_{660} are the temperature difference across the internal boundary layer and the boundary layer thickness, respectively.

the 660-km mass flux time series), whereupon it drops sharply and then rises again to an apparently critical value near 700, whereafter the next avalanche occurs. In this diagnostic analysis the temperature difference across the boundary layer is denoted by ΔT_{660}. The width of the thermal boundary layer, δ_{660}, significantly influences the variation of the boundary layer Rayleigh number ($Ra_{660} = g\alpha\Delta T_{660}\delta_{660}^3/\kappa\nu$), suggesting (which *Solheim and Peltier* [1994a] did suggest on this basis) that the avalanche phenomenon is controlled by a thermal instability of the boundary layer and that a linear stability analysis might be devised to explain the onset of such events. The purpose of this paper is to provide a detailed assessment of the ability of an analysis of this kind to explain the observed "avalanche effect".

In the following section of the paper we briefly discuss the formalism that we shall employ to analyze the stability of mean states that are characterized by the presence of an internal thermal boundary layer. The formalism will be presented for both Cartesian plane layer and spherical geometry, it being important to establish whether or not the results obtained are sensitive to this characteristic of the physical problem. Subsequent sections include a discussion of the results obtained through application of the formalism and a summary and conclusions.

Theoretical Formulation

Subject to the usual Boussinesq approximation, the nondimensional equations for mass, momentum, and energy conservation, along with a linearized equation of state, assume the following respective forms:

$$\nabla \cdot \mathbf{u} = 0, \tag{1}$$

$$\frac{Ra}{Pr}\frac{D\mathbf{u}}{Dt} = -\frac{\rho\mathbf{k} + \nabla p}{\delta} + \nabla^2\mathbf{u}, \quad (2)$$

$$Ra\frac{DT}{Dt} = \nabla^2 T + Q, \quad (3)$$

$$\rho = 1 - \delta(T - T_0). \quad (4)$$

The nondimensionalization employed in deriving this system is one in which length, time, velocity, temperature, pressure, and density are expressed as: $x_{\text{dim}} = dx$, $t_{\text{dim}} = (\nu/g\alpha\Delta T d)t$, $\mathbf{u}_{\text{dim}} = (g\alpha\Delta T d^2/\nu)\mathbf{u}$, $T_{\text{dim}} = \Delta T T$, $p_{\text{dim}} = g\alpha dp$, and $\rho_{\text{dim}} = \rho_0\rho$, respectively. Here the subscript dim refers to a dimensional quantity, g is the acceleration due to gravity, ρ_0 is a reference density, d is the characteristic length scale, ΔT is the temperature change across the boundary layer and the characteristic temperature scale, ν is the kinematic viscosity, κ is the thermal diffusivity, and α is the thermal expansivity. The thermodynamic and transport coefficients are herein assumed to be constant. $Ra = (g\alpha\Delta T d^3/\nu\kappa)$ is the Rayleigh number, $Pr = \nu/\kappa$ is the Prandtl number, $\delta = \alpha\Delta T$, and $\mathbf{k}$ is a unit vector in the vertical direction. The Prandtl number is effectively infinite in the Earth's mantle, but effects due to finite Pr will be shown to be of interest in more general circumstances to be discussed later.

Expanding the dependent variables in the system (1)-(4) as the sum of a basic state field plus a small-amplitude perturbation as $\mathbf{u} = (\nu/g\alpha\Delta T d^2)\bar{w}\mathbf{k} + \epsilon\mathbf{u}'$, $\rho = \bar{\rho} + \epsilon\rho'$, $p = \bar{p} + \epsilon\pi$, and $T = \bar{T} + \epsilon\theta$, where ϵ is an, assumed small, ordering parameter and $\bar{w}$ is written as a dimensional quantity, we obtain the set of linear field equations (5)-(8). In our analyses, $\bar{T}$ will be taken to be a boundary layer temperature profile, some examples of which are shown in Figure 2. Internal heating Q is a function of depth and is taken to have the distribution required to maintain the boundary layer temperature profile in a steady state. Although the thermal boundary layer in the large-scale, nonlinear simulations is maintained by the background flow, this assumption will allow us to evaluate the thermal part of the boundary layer instability in isolation. In the following system the variable $\bar{w}$ is an assumed background variation of vertical velocity that we will employ to capture the boundary layer stabilizing effect of convergence within the large-scale flow in which the boundary layer is embedded.

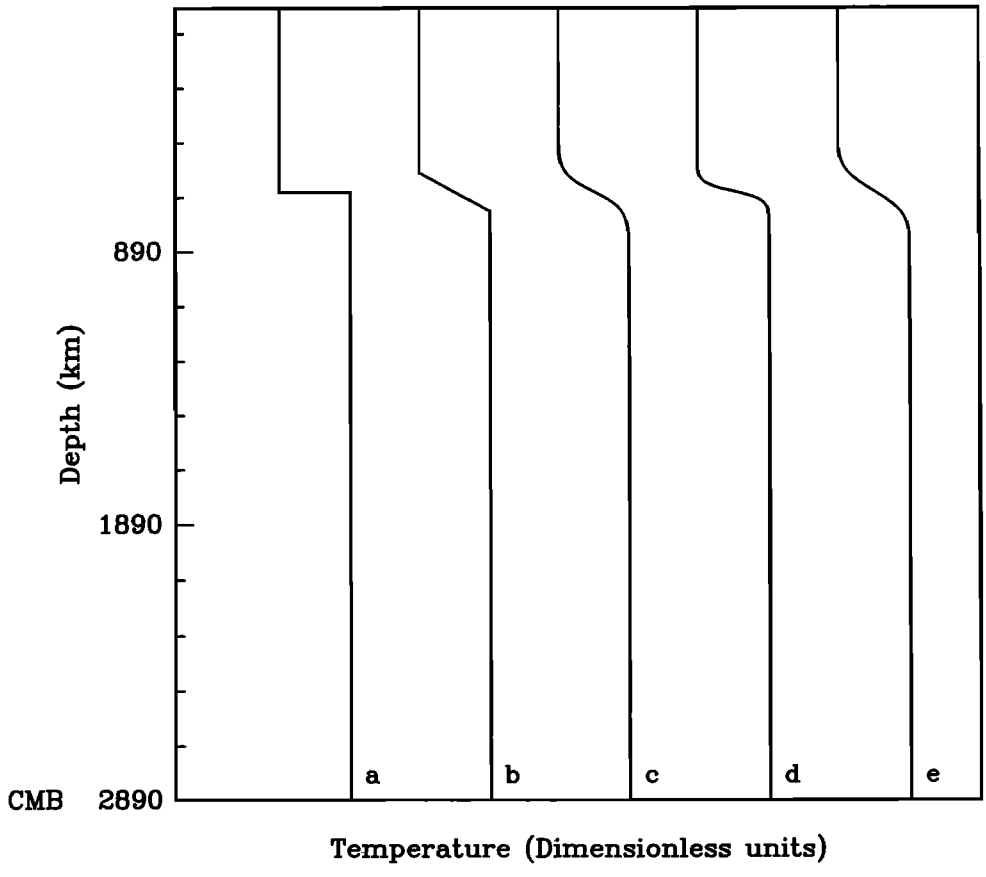

Figure 2. Temperature profiles used to approximate the boundary layer that develops at 660 km depth. The mathematical forms of the profiles are as follows with z written as a dimensional quantity: a)$T = 0$ for $z > z_0$, $T = \Delta T$ for $z < z_0$; b)$T = 0$ for $z > z_0 + 0.5\ bw$, $T = \Delta T/2 - (z - z_0)\Delta T(1/bw)$ for $|z - z_0| < 0.5\ bw$, and $T = \Delta T$ for $z < z_0 - 0.5\ bw$; c)$T = 0.5\Delta T[1 - \tanh(2.18(z - z_0)/bw)]$; d)$T = 0.5\Delta T[1 - \tanh(4.5(z - z_0)/bw)]$; and e)$T = (1.578\Delta T/\sqrt{\pi}bw)\int_0^z \exp\{-[(z' - z_0)1.578/bw]^2\}dz'$. See text for variable definitions.

$$\nabla \cdot \mathbf{u}' = 0, \tag{5}$$

$$\frac{Ra}{Pr}\frac{\partial \mathbf{u}'}{\partial t} + \frac{\bar{w}d}{\nu}(\mathbf{k}\cdot\nabla)\mathbf{u}' = -\frac{(\rho'\mathbf{k} + \nabla\pi)}{\delta} + \nabla^2\mathbf{u}', \tag{6}$$

$$Ra\frac{\partial\theta}{\partial t} + \frac{\bar{w}d}{\kappa}(\mathbf{k}\cdot\nabla)\theta + Ra\,w(\mathbf{k}\cdot\nabla)T = \nabla^2\theta, \tag{7}$$

$$\rho' = -\delta\,\theta. \tag{8}$$

In terms of the above described scaling, momentum advection scales like the Reynolds number $(\bar{w}d/\nu)$, which can be expected to be less than 10^{-22} for mantle convection and hence can be safely neglected. Temperature advection, however, scales like the Péclet number $(\bar{w}d/\kappa)$ which might be as large as 200 and will be retained in the equations. (In both cases, surface plate velocities are taken as upper bounds on $\bar{w}$). In these analyses the above defined Péclet number plays a critical role and will hereafter be referred to by v. It must be noted that the Reynolds number scales like $1/Pr$, and, as such, calculations at finite Prandtl number correspond to nonzero Reynolds number or have $v = 0$.

Substituting (8) into (6) and eliminating the pressure term in the linearized momentum balance equation by applying the operator $\nabla\times\nabla\times$ in Cartesian coordinates results in

$$\frac{-Ra}{Pr}\frac{\partial}{\partial t}\nabla^2\mathbf{u}' = \frac{\partial^2\theta}{\partial x\partial z}\mathbf{i} + \frac{\partial^2\theta}{\partial y\partial z}\mathbf{j} - \left(\frac{\partial^2\theta}{\partial x^2} + \frac{\partial^2\theta}{\partial y^2}\right)\mathbf{k} - \nabla^4\mathbf{u}'. \tag{9}$$

From the vertical component of this equation and from the previous form of the energy equation, subjecting both to Laplace transformation in time and Fourier transformation of the horizontal space coordinates, we obtain the coupled set of ordinary differential equations

$$(D^2 - k^2)(D^2 - k^2 - \frac{Ra}{Pr}\sigma)W = k^2\Theta \tag{10}$$

$$(D^2 - k^2 - Ra\,\sigma - v\,D)\Theta = W\,Ra\,DT. \tag{11}$$

In this system, D denotes d/dz, $k^2 = k_x^2 + k_y^2$ and σ is the growth rate. W and Θ are the z dependent amplitudes of the perturbation vertical velocity and temperature, respectively. Substitution for Θ from (10) into (11) yields the following modified form of the usual sixth-order ordinary differential equation in W alone in which the Péclet number v appears as a parameter.

$$(D^2 - k^2 - Ra\,\sigma - vD)(D^2 - k^2)(D^2 - k^2 - \frac{Ra}{Pr}\sigma)W = DT\,k^2\,W\,Ra \tag{12}$$

In spherical coordinates the system of ordinary differential equations that replaces (10) and (11) may be simply shown to comprise the following:

$$[D_l - \frac{l(l+1)}{r^2}][D_l - \frac{l(l+1)}{r^2} - \frac{Ra}{Pr}\sigma](W\,r) = \frac{[l(l+1)]}{r}\Theta \tag{13}$$

$$(D_l - \frac{l(l+1)}{r^2} - Ra\,\sigma - v(\frac{r_{bw}}{r})^2\frac{\partial}{\partial r})\Theta = \frac{\partial T}{\partial r}W. \tag{14}$$

In this system we have employed the notation $D_l = \partial^2/\partial r^2 + (2/r)\partial/\partial r$, in which l is spherical harmonic degree and r_{bw} is the radius of the boundary layer at midpoint. We will also find it useful in what follows to have equations relating the normal stress π to Θ and W, the vertical structure functions for temperature and vertical velocity, respectively. These relations may be obtained by taking the divergence of (6) which, in Cartesian coordinates, delivers

$$D\Theta = (D^2 - k^2)\frac{\pi}{\delta} \tag{15}$$

$$D(D^2 - k^2 - \frac{Ra}{Pr}\sigma)W = k^2\frac{\pi}{\delta}. \tag{16}$$

Boundary Conditions

Outer boundaries of the domain of analysis to be employed in what follows will always be taken to be isothermal, free-slip, and impermeable. These conditions imply that $\Theta = 0$, $D^2W = 0$, and $W = 0$ on these boundaries. In many cases the isothermal condition may be satisfied by requiring that $D^4W = 0$ on boundaries in the usual way. For some purposes it will be found interesting to consider circumstances in which the outer boundaries are placed at infinity. In these cases, W, D^2W, and Θ were required to tend asymptotically to 0 as a function of increasing distance from the internal boundary layer. This condition will be satisfied in what follows by matching an inner solution to decaying solutions of the governing equations with $DT = 0$ at a point sufficiently distant from the region of strong vertical temperature gradient. We will also find it useful in what follows to consider basic state vertical temperature variations characterized by a delta function in vertical temperature gradient (see Figure 2a). On the basis of continuity of mass, horizontal velocity, tangential stress, normal stress, and temperature, it can be shown that W, DW, D^2W, π/δ, and Θ must be continuous across a delta function temperature gradient. To find the appropriate sixth boundary condition required in this situation, we integrate (11) with $DT = -\delta(z - z_0)$ across an infinitesimally thin layer containing the delta function. Given the previously stated five continuity conditions, we thereby obtain a jump condition on $D\Theta$ such that

$$D\Theta_1 - D\Theta_2 = -Ra\,W(z_0). \tag{17}$$

In this expression the subscript 1 refers to the upper layer, while the subscript 2 refers to the lower layer, and z_0 refers to the vertical position of the boundary layer.

Rayleigh-Taylor Instability

We have found in several of the analyses to follow that results from a simpler Rayleigh-Taylor instability

analysis are instructive when compared with the results of the thermal instability analysis. The Rayleigh-Taylor stability equations may be derived from the governing equations in the usual way, following *Chandrasekhar* [1961]. They can also be derived from the above discussed thermal stability model by taking the thermal diffusivity to vanish, resulting in an infinite Rayleigh number. Subject to this assumption, (11) becomes simply

$$-\sigma\Theta = W\,DT. \tag{18}$$

Which implies that

$$\rho' = -W\frac{D\rho}{\sigma}. \tag{19}$$

Substitution of this result into (10) then delivers

$$(D^2 - k^2)(D^2 - k^2 - \frac{g d^3 \delta}{\nu^2}\sigma)W = k^2 W \frac{D\rho}{\sigma\delta}. \tag{20}$$

The growth rate may next be rescaled as $\sigma' = \delta\sigma$ in order to eliminate the parameter δ and this results in the following equation for the onset of Rayleigh-Taylor instability:

$$(D^2 - k^2)(D^2 - k^2 - \frac{g d^3}{\nu^2}\sigma')W = k^2 W \frac{D\rho}{\sigma'}. \tag{21}$$

Phase Transitions

Univariant phase transitions will be included in our analysis by employing the formulation first developed by *Busse and Schubert* [1971] and employed by *Schubert and Turcotte* [1971] and *Peltier* [1972] in application to the mantle convection problem. In this analysis the phase change is assumed to occur at thermodynamic equilibrium and so it must exist at a mean depth where the Clapeyron curve intersects the mean pressure and temperature profiles in the mantle. Such an equilibrium phase transition exerts its influence on convective mixing through two physical effects, namely, latent heat release and phase boundary deflection. Latent heat will be released or absorbed by material passing through the phase boundary, depending upon whether the transition is exothermic or endothermic, causing a vertical motion inhibiting or vertical motion enhancing effect on the material owing to the influence of thermal expansion. Furthermore, since the phase transition must be assumed to remain on the Clapeyron curve if it is to remain in thermal equilibrium, heating or cooling of the phase boundary due to latent heat release and/or temperature advection will cause the phase boundary to be deflected up or down. Because of the density difference between the shallower and deeper phases, a local vertical buoyancy force will result, which will again tend either to favor or to hinder instability. In the following formulation these effects will be taken into account using effective boundary conditions across the equilibrium position of the phase transition, assuming the phase transition to be univariant.

The additional parameters α, k, c_p, and μ will be assumed for present purposes to be the same in both phases. At the level of approximation at which we shall work, the density difference between the phases will be taken into account only when considering the buoyancy force resulting from the phase boundary deflection. W, DW, D^2W, and Θ are taken to be continuous across a phase boundary owing to the constraints of conservation of mass, continuity of tangential velocity and tangential stress and the assumption that the background temperature field is in equilibrium. The latent heat release per unit time at the phase boundary must be balanced by a discontinuity of the perturbation temperature gradient. When appropriately nondimensionalized, this delivers the following jump condition on $D\Theta$:

$$D\Theta_1 - D\Theta_2 = R_Q W. \tag{22}$$

In this equation, subscript 1 denotes the region above the phase boundary and subscript 2 denotes the region below the phase boundary. In (22) the phase change Rayleigh number is just $R_Q = (g\alpha d^3 \gamma T \Delta\rho/\kappa\nu c_p \rho^2)$. Phase boundary distortion effects are taken into account by imposing a discontinuity in perturbation pressure that is sufficient to balance the buoyancy induced by the phase boundary deflection. In nondimensional form this balance yields the second jump condition

$$\frac{\pi_1 - \pi_2}{\delta} = S\,\Theta, \tag{23}$$

in which $S = ([\Delta\rho/\rho]/\alpha d[g\rho/\gamma + DT])$ is the ratio of the phase change density contrast to the thermally induced density contrast. In the case of the Rayleigh-Taylor instability this phase boundary deflection equation may be written in the more appropriate form

$$\frac{\pi_1 - \pi_2}{\delta} = S\frac{D\rho}{\sigma'}W. \tag{24}$$

Numerical Methodology

Two different methods will be employed in what follows to solve for the critical Rayleigh numbers, growth rates, and eigenfunctions required to characterize the stability of the basic states that will be of interest to us. The first of these is a shooting method in which a Runge-Kutta-Verner scheme (as implemented in the International Mathematics and Statistics Libraries, Inc. software package) is used to integrate three linearly independent solutions satisfying the lower boundary conditions from the lower boundary to the middle of the region of strong radial temperature gradient, while three additional linearly independent solutions satisfying the upper boundary conditions are integrated down to the center of the region of strong temperature gradient. In order to implement this conventional "shooting" method, the sixth-order system was written as a set of six simultaneous first-order equations, in the form

$$\mathbf{y}' = \mathbf{A}\mathbf{y}, \tag{25}$$

where $\mathbf{y}$ is the solution vector, $\mathbf{y}'$ is its vertical derivative, and $\mathbf{A}$ is a matrix of coupling coefficients. When phase transitions are included in the model it is most convenient to include π and Θ explicitly in $\mathbf{y}$. The solution vector $\mathbf{y}$ is then taken to be

$$\mathbf{y} = (W, \quad W', \quad W'', \quad \tfrac{\pi}{\delta}, \quad \Theta, \quad \Theta').$$

If boundaries are at finite distances, appropriate linearly independent starting vectors satisfying the boundary conditions at the top and bottom boundaries may be taken to be

$$\mathbf{y_1} = (0, \quad 1, \quad 0, \quad 0, \quad 0, \quad 0),$$

$$\mathbf{y_2} = (0, \quad 0, \quad 0, \quad 1, \quad 0, \quad 0),$$

$$\mathbf{y_3} = (0, \quad 0, \quad 0, \quad 0, \quad 0, \quad 1).$$

When the outer boundaries are at infinity, starting vectors must contain decaying solutions of the equations(10,11,16) with $DT = 0$, since the DT profiles are always assumed to be localized to an internal boundary layer region.

The matrix $\mathbf{A}$ is simply derived from (10),(11), and (16) and in its most general form (in Cartesian coordinates) is

$$\begin{pmatrix} 0 & 1 & 0 & 0 & 0 & 0 \\ 0 & 0 & 1 & 0 & 0 & 0 \\ 0 & k^2 + \frac{Ra}{Pr}\sigma & 0 & k^2 & 0 & 0 \\ -(k^2 + \frac{Ra}{Pr}\sigma) & 0 & 1 & 0 & 1 & 0 \\ 0 & 0 & 0 & 0 & 0 & 1 \\ Ra\,DT & 0 & 0 & 0 & k^2 + Ra\,\sigma & v \end{pmatrix} \tag{26}$$

In order to calculate the locus of neutral stability in Ra-k space, σ is set to 0 based on the assumed validity of the exchange of stabilities principle and Ra is varied with k fixed until a linear combination of the solutions that match across the inner boundary is found. The lowest such value of Ra is the critical Rayleigh number for that wavenumber. In circumstances in which growth rates are calculated explicitly, Ra is fixed and σ is varied. In spherical coordinates the coupling matrix required to calculate the neutral curve is

$$\begin{pmatrix} 0 & 1 & 0 & 0 & 0 & 0 \\ 0 & 0 & 1 & 0 & 0 & 0 \\ \frac{-L}{r^3} & \frac{L}{r^2} & -\frac{3}{r} & \frac{L}{r} & 0 & 0 \\ \frac{-L}{r^3} & \frac{2}{r^2} & \frac{1}{r} & 0 & 1 & 0 \\ 0 & 0 & 0 & 0 & 0 & 1 \\ Ra\frac{1}{r}DT & 0 & 0 & 0 & \frac{L}{r^2} & \frac{-2}{r} + v(\frac{r_{bw}}{r})^2 \end{pmatrix}. \tag{27}$$

In (27), $L = (l(l+1))$. In spherical coordinates, Wr is employed in place of W. The shooting method, based on (25), has the advantages that it is relatively simple to implement and temperature gradients of any functional form can be investigated in either Cartesian or spherical geometry. For certain problems, however, the system of equations becomes numerically stiff, and it is found advantageous to circumvent the need to employ the numerical ordinary differential equation (ODE) solver.

In these cases a finite region of constant temperature gradient will be used to characterize the basic state (Figure 2b). Since it was found that the exact form of the gradient is not important, the necessity to employ this assumption to combat "stiffness" is not a major drawback. Under the assumption of a piecewise constant temperature gradient, the sixth-order system has constant coefficients and solutions of the form $\exp(qz)$ can be found both inside and outside the boundary layer region. The solutions outside the region of nonzero gradient are the same as those employed as starting vectors when using the shooting method with boundaries at infinity. The equation to be solved for q inside the region of nonzero gradient is simply

$$(q^2 - k^2)(q^2 - k^2 - Ra\,\sigma - v\,q)(q^2 - k^2 - \frac{Ra}{Pr}\sigma)$$

$$= -k^2\,Ra\,(\frac{d}{bw}). \tag{28}$$

In this algebraic equation the parameter bw is just the dimensional thickness of the boundary layer. When there is no background flow($v = 0$), this equation reduces to a cubic in ϕ upon substitution of $\phi = (q^2 - k^2)$ and the six complex roots can be determined analytically using Cardan's formula. When v is nonzero, the roots may be simply found numerically using Laguerre's method. When this method was employed, v was required to be a constant. As previously discussed, we will be employing the parameter v to model the influence of a basic state flow convergence onto the internal boundary layer, and for this purpose we will simply assume v to be a negative constant for $z > z_0$ and a positive constant for $z < z_0$. A matrix equation containing the boundary conditions may then be constructed and critical Rayleigh numbers and growth rates calculated by finding the zeros of the determinant of this matrix. Very similar procedures to these are used to solve for the most unstable modes in the Rayleigh-Taylor problem. The only difference in this case is that the system is then fourth order, and only growth rates can be determined because density inversions are always unstable in the absence of the influence of thermal diffusivity effects.

In what follows we will first employ the above discussed theoretical methodology to present a number of issues concerning the problem of thermal boundary layer instability in general. Following this, we will address in successive sections the problem of the stability of the internal boundary layer that appears to develop in the mantle convective circulation under the influence of the endothermic phase transition at 660 km depth.

Results

Although linear stability analysis is most often applied to the thermal convection problem in the analysis of the stability of the state of rest, the same meth-

ods have also been applied to investigate the stability of more general boundary layer temperature profiles in order to better understand the onset of secondary instabilities in the thermal boundary layers that develop in high Rayleigh number convective flows [e.g., *Howard*, 1964; *Yuen, et al.*, 1981]. As originally pointed out by *Howard* [1964], however, a thin boundary layer is most unstable for vanishingly small local Rayleigh number and at very large wavelength.

Thermal Boundary Layer Stability

In order to explicitly validate *Howard*'s [1964] comment, neutral curves were calculated for a boundary layer of fixed thickness located in the middle of a fluid region as a function of the total layer depth L. The results of these analyses are shown in Figure 3a for the sequence $(L/bw) = 4, 6, 8, 10, \infty$. For the purpose of these analyses the governing equations were scaled by the thickness of the boundary layer bw. Curves of neutral stability do not depend on the Prandtl number, and the Péclet number is set to 0. Effects due to finite Péclet number will be discussed in a later section. In this calculation and for all other calculations to be presented, the temperature gradient is taken to be piecewise constant unless otherwise stated. The region above a neutral curve denotes the region of Rayleigh number-wavenumber space in which the growth rate is positive and in which a fluctuation will therefore grow in time. The minimum in this curve $Ra_{\min}$ denotes the lowest Rayleigh number above which instability is possible, and the horizontal wavenumber $k_{\min}$ at which this minimum is realized denotes the horizontal wavenumber of the so-called fastest growing mode of linear instability. It will be noted from Figure 3a that as the outer boundaries are moved progressively farther from the region of nonzero temperature gradient, $Ra_{\min}$ and $k_{\min}$ both rapidly approach zero. The lowest curve, corresponding to the circumstance in which the boundaries are placed at infinity, never recovers for small k. This may seem surprising in that it appears that a vanishingly small temperature gradient can cause the onset of a very large scale instability in a thick layer of fluid. However, it is important to realize that in a thick layer there will be considerable gravitational potential energy available to drive instability owing to the large thickness of fluid of higher density overlying an equally great thickness of fluid of lower density. When $Ra_{\min}$ and $k_{\min}$ are plotted as a function of the ratio bw/L, (long-dashed line and short-dashed line in Figure 4a, respectively), an interesting scaling emerges. $Ra_{\min}$ is seen to scale like $(bw/L)^3$ for L sufficiently greater than bw, while k scales like (bw/L) itself. This implies that the natural length scale for the system is, in fact, the entire layer depth L and that if this nondimensionalization is chosen, the dynamics do not vary with bw for

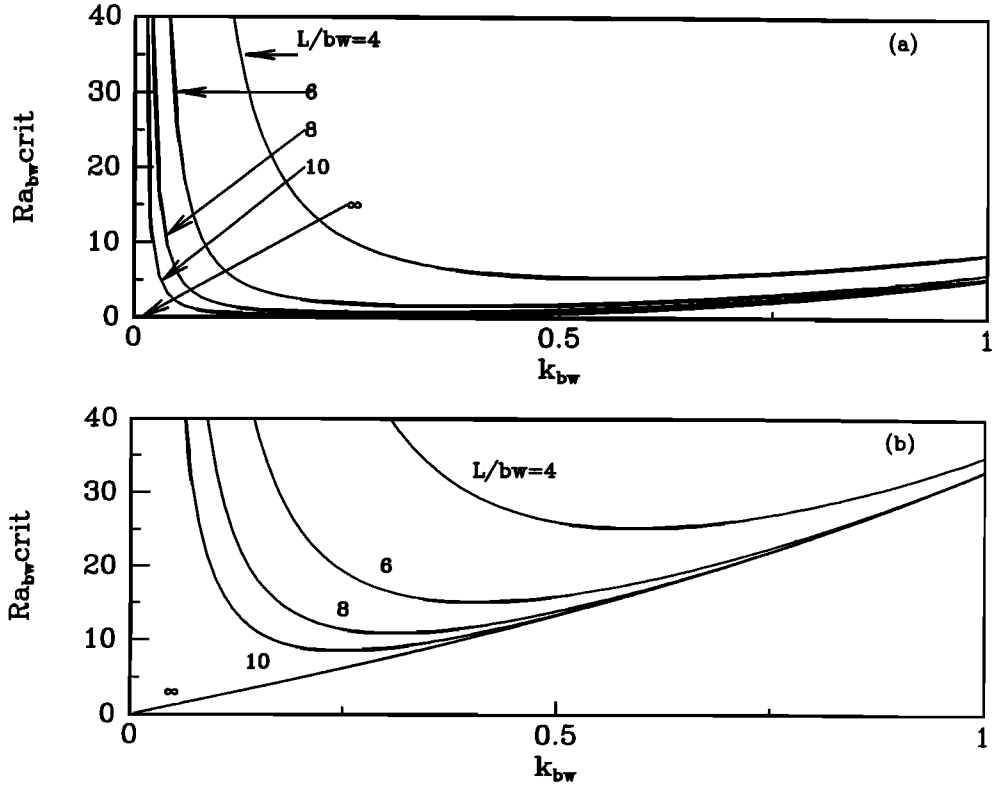

Figure 3. (a) Neutral curves with quantities scaled by bw and differing distances to outer boundaries with the boundary layer placed at the center of the fluid region. From top to bottom, L/bw=4,6,8,10, and ∞. (b) Neutral curves with quantities scaled by bw and differing distances to the far outer boundary with the boundary layer adjacent to one outer boundary. From top to bottom, L/bw=4,6,8,10, and ∞.

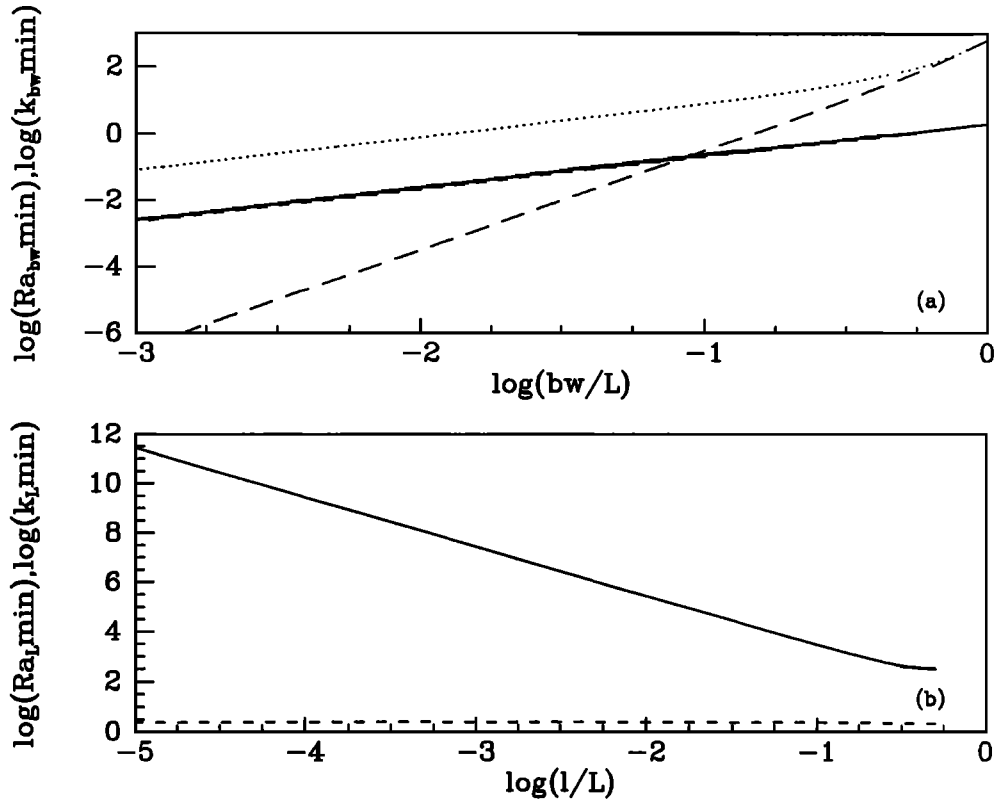

Figure 4. (a) Variation of minimum critical Rayleigh numbers and wavenumbers with $\log(bw/L)$. Long-dashed lines are Rayleigh numbers for a boundary layer placed in the middle of a fluid region. Short-dashed lines are wavenumbers for a boundary layer placed in the middle of a fluid region. Dotted lines are critical minimum Rayleigh numbers for the case in which the boundary layer is adjacent to an outer boundary. Solid lines are minimum wavenumbers for the case in which the boundary layer is placed adjacent to an outer boundary. b)Variation of $\log(Ra_{L\min})$ (solid line) and $\log(k_{L\min})$ (dashed line) with $\log(l/L)$ using a delta function temperature gradient.

bw/L sufficiently small. Nondimensional quantities will henceforth have subscripts indicating the length scale by which they are nondimensionalized.

Figure 5 shows the variation of $Ra_{L\min}$ with bw/L for a boundary layer placed in the middle of the fluid region. The three curves shown are for three different mathematical forms of the boundary layer temperature gradient, including a step function, a hyperbolic secant squared, and a Gaussian. These are, respectively,

$$DT = -L/bw \text{ for } |z - z_0| < 0.5(bw/L),$$
$$DT = 0 \qquad |z - z_0| > 0.5(bw/L) \tag{29a}$$

$$DT = -2.18L/(2bw)\mathrm{sech}^2[2.18(z - z_0)L/bw] \tag{29b}$$

$$DT = -1.578L/(bw\sqrt{\pi})\exp(-\{[1.578(z - z_0)L]/bw\}^2). \tag{29c}$$

The corresponding temperature profiles are shown in Figures 2b, 2c, and 2e. Inspection of the results shown in Figure 5 demonstrates that for bw/L less than 0.1, $Ra_{L\min}$ is independent both of bw and of the exact form of the temperature gradient. When $bw = L$ for the step function case, we recover the Rayleigh-Bénard critical value of 657.51, and when bw=0, the minimum Rayleigh number of 327.39 obtains, which is the critical Rayleigh number for a delta function temperature gradient situated in the middle of a layer of unit thickness. This quantity was found to be quite useful in that it provides a convenient check on any thin boundary layer in the middle of a plane layer. Since most boundary layers of interest will be considerably thinner than the entire fluid region in which they are found, it is seen that a thermal boundary layer in the middle of a deep fluid region may be well approximated by a delta function temperature gradient. It will also be shown presently that a thin thermal boundary layer at arbitrary depth in a layer of finite thickness is well approximated by a delta function at the appropriate depth. Also of interest is the fact that $Ra_{L\min}$ is a monotonically increasing function of bw/L, implying that thin regions of strong temperature gradient in the middle of deep layers are more unstable than thick regions. This makes good physical sense since thin regions of strong gradient are associated with greater temperature contrast between the upper and lower regions of the fluid, resulting in greater buoyancy forces. Minimum critical horizontal wavenumbers k_L were found to vary only slightly with

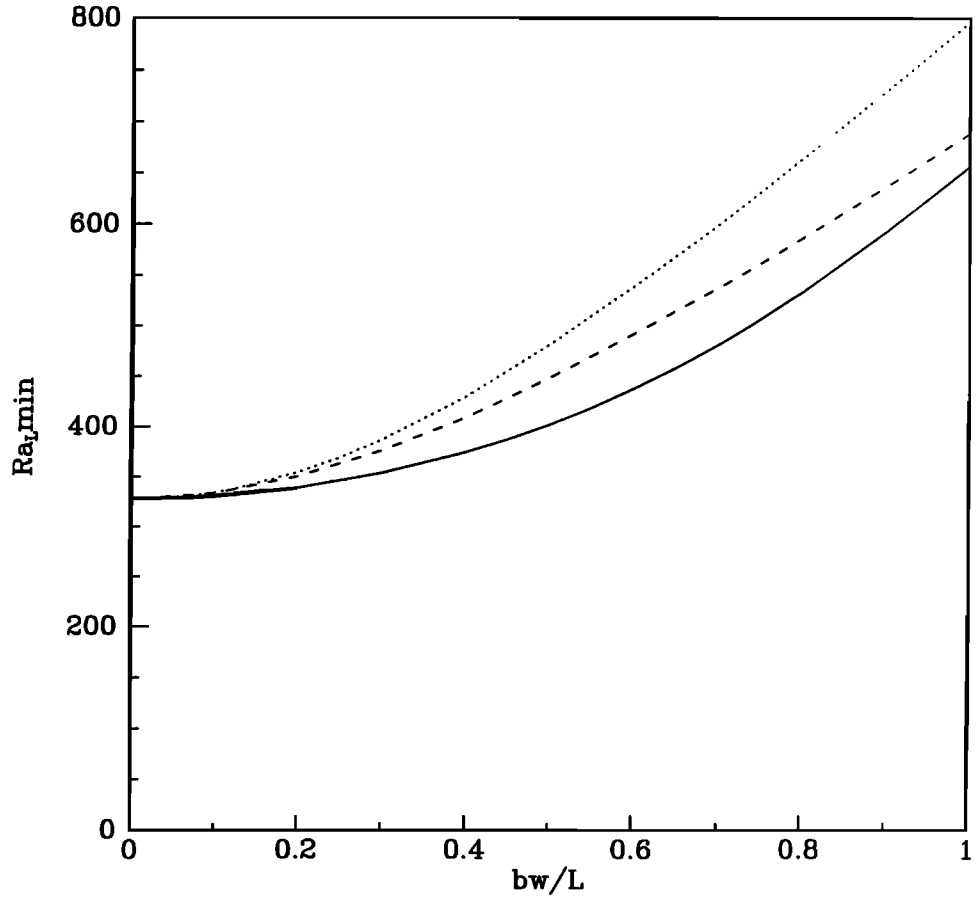

Figure 5. Variation of minimum Ra_L with bw/L, based upon the following alternative choices for the profile of temperature gradient: $DT = -1.578L/(bw\sqrt{\pi})\exp\{-[(z-z_0)1.578L/bw]^2\}$(dotted line), DT=-2.18L/(2bw)sech^2[2.18$(z-z_0)L/bw$](dashed line), and $DT = -L/bw$ for $|z-z_0| < 0.5\ bw/L$ and $DT = 0$ for $|z-z_0| > 0.5\ bw/L$ (solid line).

bw/L , decreasing monotonically from 2.227 to 2.221 as bw/L was increased from 0 to 1.

Figure 6a shows vertical velocity W (solid line) and temperature perturbation Θ (dotted line) eigenfunctions and eddy heat transport $< \Theta W >$ (dashed line) for the delta function temperature gradient in the middle of a plane layer. We see that the vertical velocity eigenfunction is virtually unchanged from the solution of the Bénard (constant gradient) case (Figure 6b), and all of the vertical structure functions are seen to fill the entire region; they are in no way limited to the boundary layer region of space. Also, because the horizontal wavenumber does not change significantly, the aspect ratio of the convection cells changes very little with bw/L. For the case of a localized gradient in the middle of a plane layer, we note that *Howard*'s [1964] predictions are simply a consequence of the fact that the natural length scale of the system is the entire layer depth. Since $k_{bw} = k_L(bw/L)$ for a given physical configuration and $Ra_{bw} = Ra_L(bw/L)^3$ and given that k_L and Ra_L both tend to constants for $bw/L << 1$, it is clear that $k_{bw\min}$ and $Ra_{bw\min}$ must be vanishingly small for $bw << L$. That the temperature perturbation eigenfunction develops a cusp and, as such, is narrowed by the narrower boundary layer will be seen to be important in determining the stability of a boundary layer in the presence of a phase transition.

Referring to the previously discussed Figure 3b, we present a series of neutral curves for variables scaled by the boundary layer thickness, when the boundary layer is located adjacent to one of the impermeable boundaries for various total layer depths. As in Figure 3a, we present results for the sequence L/bw=4,6,8,10 and ∞. Again, the critical Rayleigh number and wavenumber go to zero as the outer boundary is moved progressively farther away. *Yuen et al.* [1981] presented growth rate curves nondimensionalized by the boundary layer depth for a boundary layer at the surface of an infinite half-space. Their results for constant viscosity were qualitatively reproduced in the course of this investigation. Of interest is the fact that their growth rate curve does not have a long-wavelength cutoff, clearly indicating that $Ra_{bw\min}$ must go to zero as k goes to zero. One might expect that a boundary layer located adjacent to an impermeable boundary would be less unstable than a boundary layer well removed from walls because most of the fluid region would be isothermal, with only a small region of density contrast on

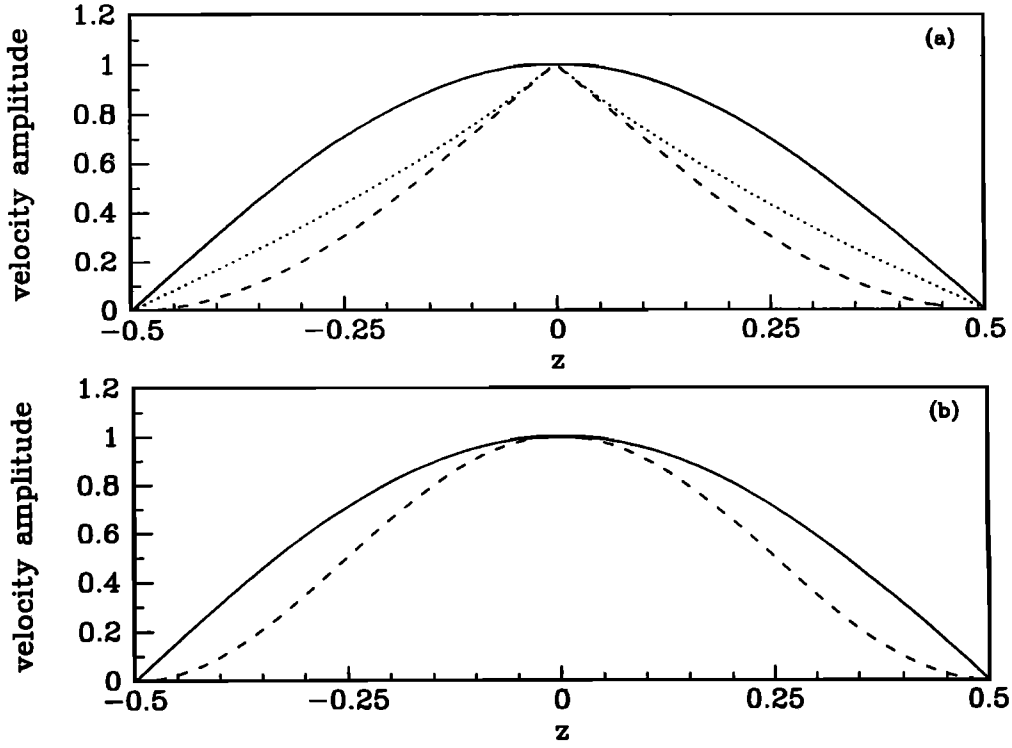

Figure 6. (a) Eigenfunctions for the case in which the governing equations are scaled by the total layer depth and a delta function temperature gradient is assumed. Solid line is the vertical velocity eigenfunction, dotted line is the temperature perturbation eigenfunction, and the dashed line is the eddy heat transport. (b)Eigenfunctions for the case in which the governing equations are scaled by the total layer depth for the case of a constant temperature gradient (Bénard configuration). Solid line is the vertical velocity and the temperature perturbation eigenfunctions (they are identical in this case); dashed line is eddy heat transport. Note that all eigenfunctions have been normalized so that their peak amplitudes are unity.

one extremity. This is found to be the case in that the Rayleigh number is seen to approach 0 as bw/L in this case (dotted line in Figure 4a) rather than as $(bw/L)^3$, which is the scaling for a boundary layer in the middle of a deep layer. The solid line in Figure 4a shows the scaling of $k_{bw\min}$ when a boundary layer is located adjacent to an outer boundary. This result implies that if the equations were scaled by the entire layer depth, the critical Rayleigh number would, in fact, diverge to infinity as $(L/bw)^2$ for $bw << L$. This was found to be the case. From Figure 4b it will be noted that if a delta function gradient is moved toward the edge of a unit layer, $Ra_{L\min}$ diverges inversely as the square of the distance to the closest outer boundary, the same scaling that obtains when a finite thickness boundary layer adjacent to a single horizontal boundary is decreased in thickness. This indicates that it is not the depth of the region of strong gradient that is important but, rather, the distance from the effective center of the region of strong gradient to the nearest impermeable boundary. This length scale we will henceforth call l. The results shown in Figure 4b may be employed to determine the minimum critical Rayleigh number for any thin boundary layer in a deep fluid region by locating the relative position of the boundary layer in the layer, determining the corresponding Rayleigh number and then scaling the result appropriately. Also of interest is that the eigenfunctions remain "space filling" when the thermal boundary layer is located adjacent to an impermeable boundary and, furthermore, since the horizontal wavenumber (dashed line Figure 4b) is seen to vary very little with l/L, the aspect ratio of the cells remains of order unity.

Some calculations of growth rates with supercritical Rayleigh numbers were performed with equations scaled by bw and with various distances to outer boundaries and with various values of the Prandtl number. In each case the Péclet number v was set to 0. In particular, it was observed that at infinite Prandtl number the wavelength of the most unstable mode once again scaled with the distance to the nearest outer boundary and diverged if the outer boundaries were placed infinitely far away from the thermal boundary layer region. If a finite Prandtl number was used and, as such, the inertial term was included in the equations, it was observed that even for outer boundaries at infinite separation, the disturbance occupied only a finite region of space. The new length scale imposed under these circumstances was seen to be $(\nu^2/g)^{\frac{1}{3}}$.

Application to Convection in the Earth's Mantle: Initial Estimates

In order to compare the critical boundary layer Rayleigh numbers inferred from the nonlinear, time depen-

dent simulations of *Solheim and Peltier* [1994a, b] to those arising from a purely thermal instability, the equations were scaled by 140 km, a typical boundary layer thickness obtained in the *Solheim and Peltier* [1994a] simulations of the influence of phase transitions on convective mixing. The boundary layer was then placed so as to be centered on 660 km depth, and the free-slip outer boundaries were placed in accordance with the scaled positions of the core-mantle boundary (CMB) (dimensional depth of 2890 km) and the Earth's surface. The minimum Rayleigh numbers that were obtained in Cartesian and spherical coordinates were 0.0773 and 0.0819, respectively, for this circumstance and these obtained at dimensional wavelengths of 8000 and 7800 km, respectively. (See the lowest neutral curve in Figure 7a for the Cartesian case with v=0). The eigenfunctions were seen to fill the entire space between the lower and upper boundaries (Figure 7b shows the vertical velocity (solid line) and temperature perturbation (dotted line) eigenfunctions). This solution clearly represents what we might refer to as an avalanche since it does involve the entire depth of the fluid and its horizontal wavelength is of the order of the wavelengths of the observed avalanche disturbances, which were typically seen to be about 8000 km. The minimum Rayleigh number, however, is many orders of magnitude smaller than those observed by *Solheim and Peltier* [1994a]. Although a very small boundary layer Rayleigh number is to be expected for this geometry based on the discussion of the previous section, the question as to why the thermal boundary layer in Figure 1 is not unstable at much lower Rayleigh numbers clearly arises.

An important issue certainly concerns the influence of the phase transition itself. The parameters used to estimate S and R_Q for the spinel to postspinel phase transition at 660 km depth for this purpose are listed in Table 1. The resulting parameters, S and R_Q, based upon these parameters, were calculated to be -1.8 and -95, respectively. With this phase transition positioned at the center of the thermal boundary layer, the system was found to have a negative minimum Rayleigh number, indicating that there would need to be a stabilizing temperature gradient for the system to be even marginally stable. This clearly indicates that at onset of instability, for Earth-like geometry, the destabilizing latent heat effect of the endothermic phase transition dominates the stabilizing phase boundary deflection effect since the critical Rayleigh number is seen to decrease. This was first demonstrated by *Peltier* [1985]. *Buffet et al.* [1994] obtained a similar result for the case of a linear temperature profile throughout the mantle. In order to test the robustness of this result, the stabilizing parameter S was increased in magnitude, with fixed R_Q, until the Rayleigh number became positive. The

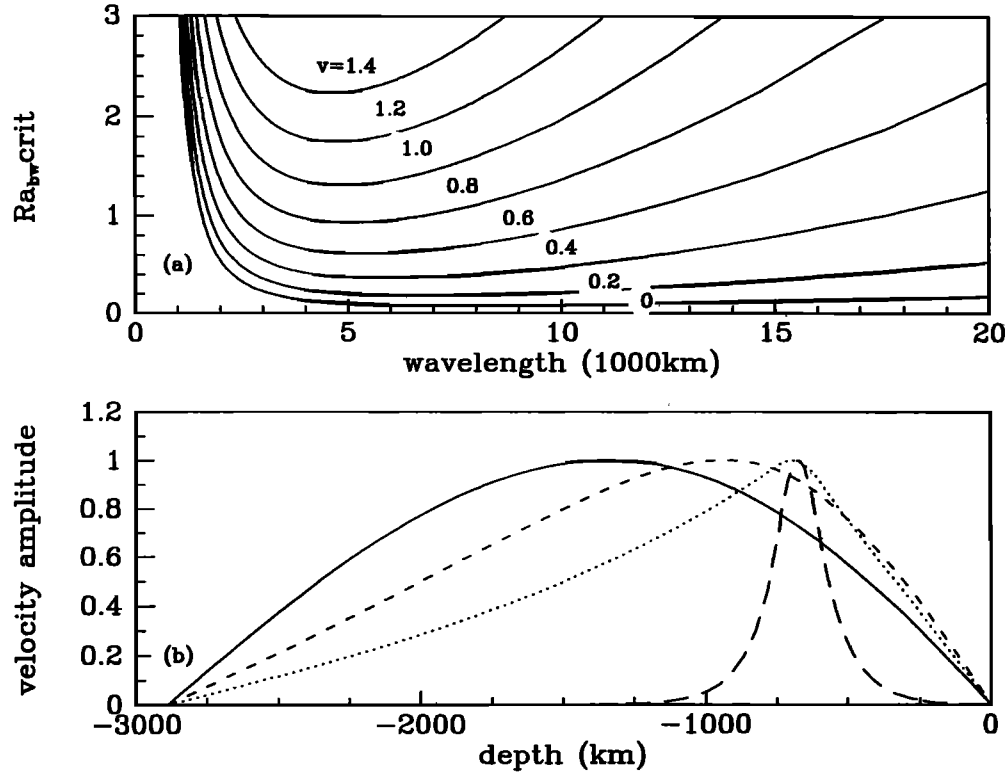

Figure 7. (a) Neutral curves for the case in which the boundaries are placed to coincide with the Earth's surface and core-mantle boundary (CMB), with no phase change present but with a background velocity convergence onto the boundary layer at 660 km depth. From bottom to top v=0, 0.2, 0.4, 0.6, 0.8, 1.0, 1.2, and 1.4. The stabilizing influence of a velocity convergence is clearly demonstrated. (b) Vertical velocity eigenfunctions with v=0 and v=1.4 (solid line and short-dashed line, respectively) and temperature perturbation eigenfunctions for v=0 and v=1.4 (dotted line and long-dashed line, respectively).

Table 1. Representative Values of the Parameters of the 660-km Phase Transition

Parameter	Symbol	Value
Density difference between lower and upper phases	$\Delta\rho$	450 kg/m^3
Average density	ρ	4200 kg/m^3
Characteristic length scale	d	140 km
Thermal expansivity	α	2.5×10^{-5} K^{-1}
Gravitational acceleration	g	10 m/s^2
Clapeyron slope	γ	-2.8×10^6 kg/(m s^2 K)
Temperature gradient at the phase boundary	$DT(z_0)$	-2.14×10^{-3}K/m
Temperature at the phase boundary	T	2300 K
Kinematic viscosity	ν	10^{18}m^2/s
Thermal diffusivity	κ	9.5×10^{-7} m^2/s
Specific heat capacity at constant pressure	c_p	1250 J/(K kg)

critical value of S was thereby shown to be near -12, indicating that one could not achieve stabilization by tuning the parameters. Again, this result is not surprising given that *Peltier* [1985] pointed out that when the 660-km endothermic phase transition is placed in a layer of the dimensions of the Earth's mantle, the destabilizing influence of latent heat release dominates because it scales like L^3, while the stabilizing phase boundary deflection effect scales like $1/L$. Although the equations in this case are explicitly scaled with the narrow boundary layer thickness bw, it seems clear that the stabilizing or destabilizing nature of a phase transition cannot depend on an arbitrary choice of nondimensionalization. Since the natural length scale of the system has been demonstrated to be the "outer scale" L it would seem that an endothermic phase transition in a fluid region becomes increasingly destabilizing with the depth of the fluid region. In order to test this, an endothermic phase transition with the same parameter values for S and R_Q as above was placed in the middle of a boundary layer of depth bw in a fluid layer of depth L. The equations were nondimensionalized by bw. As (L/bw) was increased, the critical Rayleigh number varied from being well above the critical Rayleigh number in the absence of a phase transition for $(L/bw) = 1$ to negative for $(L/bw) = 3$. The nondimensional distances from the phase transition to the surface and CMB are 4.79 and 15.9, respectively. This clearly indicates that endothermic phase transitions become increasingly destabilizing with the depth of the total layer and the 660-km phase transition is very strongly destabilizing at onset for Earth geometry. This destabilization was verified for spherical geometry as well. The additional influences of the phase transition at 400 km depth were also added to the model, as in the work by *Peltier* [1972], but these were found to be only slightly stabilizing.

It has been argued [e.g., *Tackley*, 1995] that the effect of latent heat in high Rayleigh number convection is considerably less significant then in a quiescent background state. This is because a convecting fluid tends to adopt an adiabatic temperature profile, and as a result, the temperature change induced by latent heating is felt everywhere beneath the phase boundary and, as such, no buoyancy-producing lateral density gradients are created. In one series of calculations, the latent heating parameter R_Q was set to 0. For $S = -1.8$ a critical Rayleigh number of 0.1 obtained at a wavelength of 8000 km. Evidently, even in the absence of latent heating effects, the endothermic phase transition at 660 km depth will not stabilize a thermal boundary layer to the extent that stability is observed in the numerical simulations of *Solheim and Peltier* [1994a, b]. Clearly, effects other than phase transitions must be included in a linear stability calculation in order to account for the relative stability of the thermal boundary layers seen in the numerical simulations and for the importance of the boundary layer thickness in determining this stability.

Rayleigh-Taylor Analysis With a Phase Transition

A necessary criterion for penetration through an endothermic phase boundary was recently suggested by *Bercovici et al* [1993], based upon a parameter $F_r = (\rho^2\alpha g d)/(\gamma\Delta\rho)$, representing the ratio of gravitational to phase boundary deflection forces, and it was suggested that the value of this parameter should exceed 1 for penetration to occur. Since both of the forces whose balance is represented by this ratio increase linearly with ΔT, the parameter itself is clearly independent of the temperature contrast across the boundary layer but, importantly, increases with the length scale d. F_r is also the negative reciprocal of our parameter S if temperature gradient effects are neglected. In order to test the utility of this parameter in the context of a complete Rayleigh-Taylor analysis, an endothermic phase change was placed in the middle of a boundary layer and growth rates were calculated as a function of wavelength for the Rayleigh-Taylor case with equations scaled by the boundary layer thickness bw. Latent heating effects were neglected as these cannot be assessed in the absence of thermal diffusion. This process was repeated for different values of the boundary layer thickness, which resulted in different values of the parameter

S. In Figure 8a we show results for a sequence of calculations with S=-0.943, -0.962, -0.980, -1.0, -1.02, and -1.04. Vertical velocity eigenfunctions, corresponding to the most unstable modes for this sequence of analyses, are shown in Figure 8b. Inspection of these results demonstrates that the eigenfunctions change from avalanche type (layer filling) to layered type when bw is fixed such as to set the parameter S to a value close to -1. This analysis differs from that performed by *Bercovici et al.* [1993] in that these authors considered an isolated descending plug, while here we assume that the boundary layer has been built up uniformly by the background flow. The length scale used in the analysis of Bercovici et al. is the average thickness of that part of the plug which has accumulated above the phase boundary and represents the thickness of an imposed density fluctuation. In the work reported herein the length scale used to calculate S is the thickness of the region of significant background density gradient bw. However, in the absence of thermal conductivity, density fluctuations are proportional to the density gradient for an avalanche solution (see (18)) and so their thickness is fixed by the thickness of the boundary layer. The thickness of the boundary layer is thus demonstrated to be critically important in determining whether an avalanche will occur in the case of a Rayleigh-Taylor instability.

It is seen then that a mechanism does exist within the Rayleigh-Taylor formalism to turn avalanches on and off: avalanches will occur if the boundary layer is sufficiently thick. If not, the instability develops as a layered mode. The question remains, however, as to how appropriate such an analysis, based upon the neglect of thermal conduction effects, could be in describing the boundary layer instability events that could occur within the Earth's mantle. One important problem clearly arises in consequence of the fact that the growth rate calculated for the avalanche slightly below the critical value of S is such that risetimes are 2 orders of magnitude shorter than those observed in the full nonlinear simulations of *Solheim and Peltier* [1994a], which are operating in the statistical equilibrium state. Clearly, another problem is that in the Rayleigh-Taylor analysis, density inversions always drive instability; no stable regime exists of the kind that is observed in the nonlinear simulations. When in the layered regime, the instability would erase the boundary layer, which would destroy the possibility of further avalanches. As avalanches are observed in the nonlinear simulations, intermittently separated by significant periods of stably

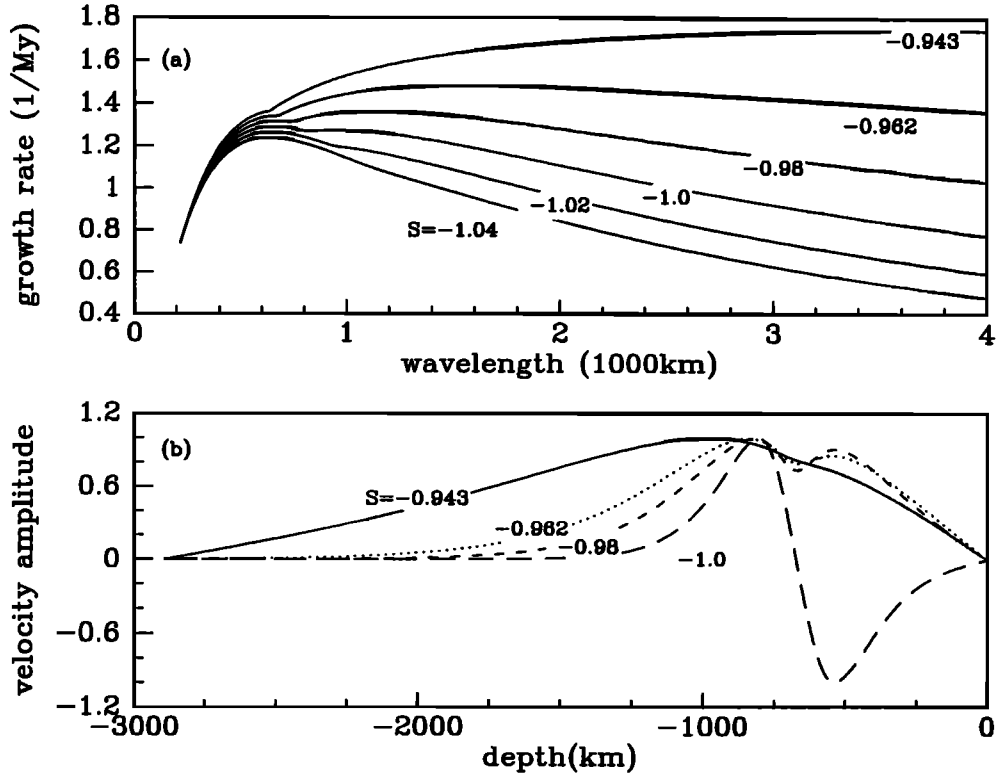

Figure 8. (a) Variation of growth rate with wavelength for Rayleigh-Taylor instabilities with outer boundaries at positions corresponding to the Earth's surface and CMB and with an endothermic phase transition at 660 km depth. Different curves correspond to different values of the stabilizing parameter S, where S=-1 is the critical value. From top to bottom, S=-0.943, -0.962, -0.98, -1, -1.02, and -1.04, and we see the transition from a short-wavelength maximum for $S < -1$ to a long-wavelength maximum for $S > -1$. (b) Vertical velocity eigenfunctions with $S = -0.943$ (solid line), $S = -0.962$ (dotted line), $S = -0.98$ (short-dashed line), and $S = -1$ (long-dashed line). Note that below S=-1 the eigenfunctions all have the same layered form.

layered flow, it seems clear that thermal diffusion effects cannot be neglected. The Rayleigh-Taylor criterion is insufficient to explain the avalanche process.

As a consequence of finite thermal diffusivity, the perturbation temperature eigenfunction of the unstable mode becomes nonlocal. As penetration through the phase boundary was demonstrated to increase with the width of the perturbation density (which is proportional to the perturbation temperature), thermal instabilities remain avalanches for much more negative values of the stabilizing parameter S. When temperature perturbation eigenfunctions were plotted along with velocity eigenfunctions (not shown) and when phase transitions were present in the thermal instability case, it was observed that temperature perturbation eigenfunctions were always nonzero over a significant region surrounding the phase boundary whenever avalanches occur. This demonstrates that although the penetrative or layered properties of convection through a phase boundary are not fixed by the boundary layer thickness and the parameter S in the thermal instability case as they are in the Rayleigh-Taylor case, the depth extent of the temperature fluctuation is vitally important in determining whether or not an avalanche will occur. For this reason, any process that results in a localization of the perturbation temperature eigenfunction will result in a stabilization of the boundary layer against the occurrence of an avalanche.

Process of Dynamical Stabilization

One important factor neglected in the previous sections concerns effects due to the background flow. More heat is advected into a boundary layer region by convective flows than is advected outward [*Jarvis and Peltier*, 1982]. Thus effects due to the background flow might quite reasonably be expected to result in a localization of a density perturbation and hence stabilize an internal thermal boundary layer in the presence of an endothermic phase transition as described in the previous section. In order to simply capture effects due to advective heat convergence by the background flow, a constant positive Péclet number will be assumed below the phase transition and an equal in magnitude constant negative value will be assumed above. As previously discussed, momentum advection due to the background flow may be neglected for mantle circulation and, as such, this velocity convergence will affect the stability of the boundary layer only through its influence on the temperature structure. This incorporation of mean flow effects through introduction of a constant velocity convergence might be expected to be justifiable on the basis of a separation of length scales in two limiting cases: (1)if the width of a thermal plume in the layered state is much larger than the wavelength of a boundary layer instability and (2)if the spacing between thermal plumes in the layered state is much less than the wavelength of a boundary layer instability. It is this second limit which we expect to be appropriate in the present context; in the simulations of *Solheim and Peltier* [1994a], avalanche instabilities are seen to have long wavelengths compared with the internal spacing of upper mantle thermal plumes. A schematic representation of this scenario is presented in Figure 9. The dashed lines represent the upper and lower extremities of the boundary layer, while the sinusoid represents an incipient instability of the boundary layer itself. One wavelength of the incipient instability extends over many upper and lower convection cells. Although there is an outward flow that is necessary to conserve mass, there is a net influx of advected heat, and it is the effects of this heat advection that we wish to capture through the Péclet number parametrization.

An upper bound on the Péclet number v, based upon surface plate velocities of the order of 4 cm/yr would be approximately 200. For the purposes of the linear stability analysis, v is expected to be much smaller however, since it is intended to represent only the effective convergence onto the boundary layer and not the total background flow. Referring once more to Figure 7a, a series of neutral curves are presented for various values of the nondimensional velocity convergence (Péclet number) in the absence of phase transitions for the Earth-like geometry described above. The minimum critical Rayleigh number is seen to rise monotonically with v. In order to attain Rayleigh numbers similar to those recorded in the *Solheim and Peltier* [1994a] analysis, v was required to be near 100. It seems unlikely that the effective background convergence for boundary layer stabilization could be of the same order of magnitude as the mean flow speed. The role of the dynamics in stabilizing the internal thermal boundary layer is, nevertheless, clearly illustrated, and it is rather likely that effects due to deformation flows that apply effective convergence across the region of strong radial temperature gradient will stabilize internal thermal boundary layers in high Rayleigh number convection. Also of interest are the perturbation vertical velocity and temperature eigenfunctions, which are shown in Figure 7b as the short-dashed line and long-dashed line, respectively, for the case v=1.4. It will be observed that the velocity structure is shifted somewhat from the zero background velocity case, but more importantly, the temperature perturbation eigenfunction becomes strongly localized into the region of the boundary layer itself.

When the endothermic phase transition is also placed in the center of the boundary layer and a background velocity convergence is active, it is found that the combination of these effects may be very strongly stabilizing indeed. Figure 10a shows a series of neutral curves for which the parameters of the endothermic phase transition are chosen to be the same as those employed above and with various values for the velocity convergence. Two distinct minima are now observed to be characteristic of the neutral curves. Figure 10b shows eigenfunctions for critical Rayleigh numbers and wavelengths corresponding to the long wavelength (8800 km,v=1.3) and short-wavelength (1375 km,v=1.4) minima. The long-wavelength solution represents an avalanche, while the short-wavelength solution represents a split mode of instability with no penetration of the phase bound-

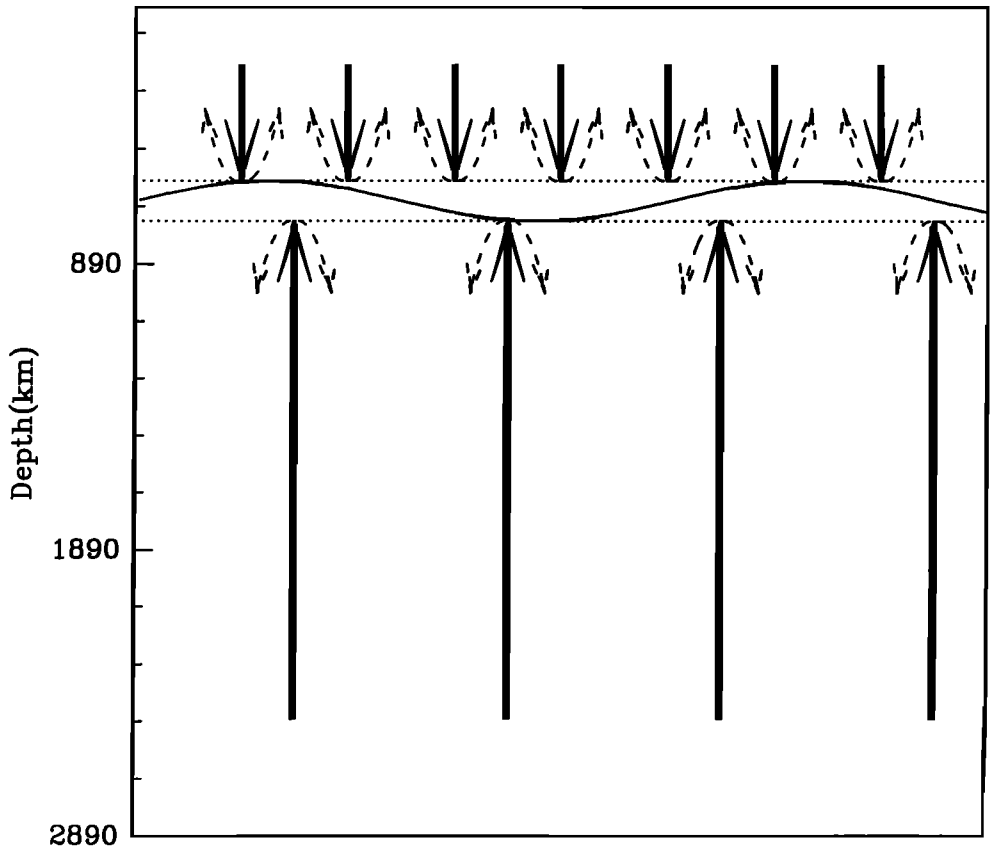

Figure 9. Schematic illustrating the process of dynamical stabilization of the thermal boundary layer. The influence of temperature advection onto the boundary layer (solid arrows) in convergence is taken to exceed the influence of advection of the return flows (dashed arrows). The spacing between thermal plumes in the layered state is considerably shorter than the wavelength of a boundary layer instability (sinusoid), supporting a separation of length scales argument whereby a simple parametrization of the background flow as a constant convergence may be employed.

ary. On the basis of the neutral curves, it is seen that if the background convergence onto the boundary layer is increased, the low-wavenumber minimum disappears and the fastest-growing instability is switched from avalanche to layered style. In nonlinear simulations an increase in the system Rayleigh number is seen to decrease the number of avalanche events, leading to more complete layering. It seems reasonable that larger external Rayleigh numbers will correspond to higher average convergence onto the phase boundary, and so this result agrees well with the numerical simulations. Our analysis clearly predicts that for very large external Rayleigh numbers the flow would be more nearly perfectly layered, a circumstance that we expect would most probably have obtained in the early Earth. It has often been suggested [e.g., *Peltier*, 1996] that such phase transition induced layering in the early Earth could have led to the development of a chemical discontinuity across the phase change interface, thus strongly increasing the degree of layering.

Figure 11a shows a series of neutral curves for a constant value of the background convergence (v=1.4) but with different values of the Clapeyron slope of the phase transition using a temperature gradient of the form $DT = -2.25\text{sech}^2[4.5(z - z_0)]$(Figure 2d). For smaller values of the magnitude of the Clapeyron slope we see that the long-wavelength avalanche solution corresponds to the most unstable mode. As the magnitude of the Clapeyron slope is increased, however, the most unstable mode changes from one with a wavelength near 8000 km to one with a wavelength near 1300 km. Clearly, there is a critical Clapeyron slope below which layering is enforced. For this particular value of the background velocity and for this form of the temperature gradient, the critical Clapeyron slope is found to be between -2.58 and -2.59 MPa/K. A critical value of the Clapeyron slope is found to exist for every value of the background velocity convergence. Note also that all of the curves are identical in the short-wavelength limit and that once the Clapeyron slope is sufficiently stabilizing, the minimum critical Rayleigh number does not increase with a further decrease in the Clapeyron slope. This value of the Rayleigh number is an upper bound on the possible value for the minimum critical boundary layer Rayleigh number for an avalanche solution for a particular velocity convergence with a boundary layer of a particular vertical structure.

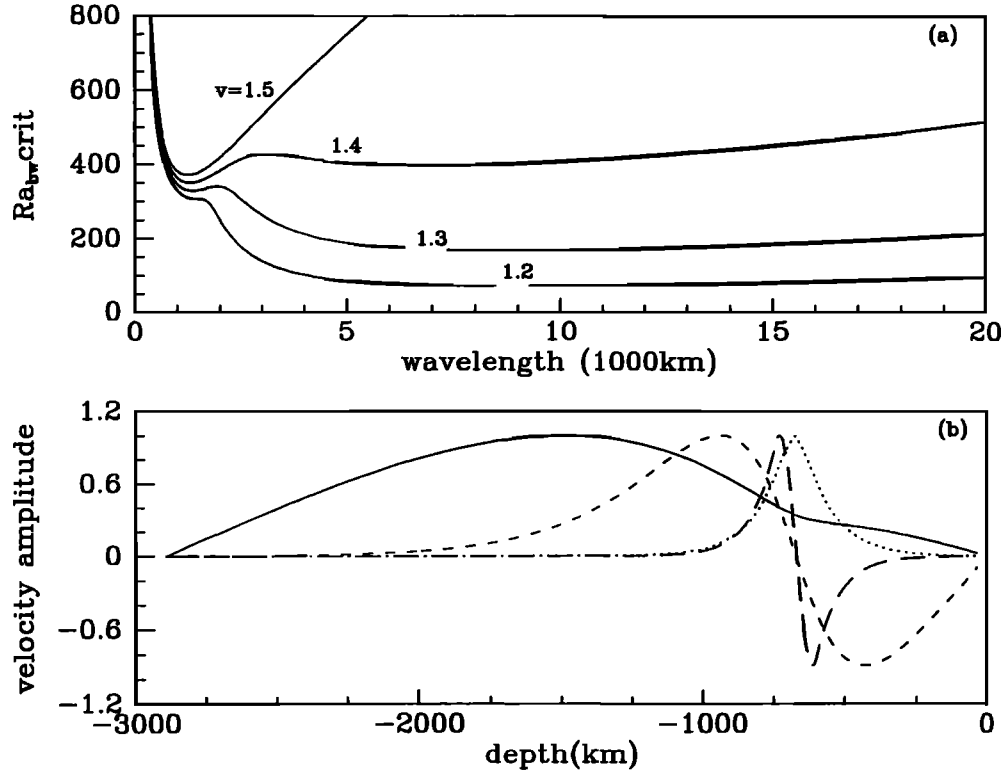

Figure 10. (a) Neutral curves with a phase transition of Clapeyron slope -2.8 MPa/K placed at 660 km depth and varying values of velocity convergence. From top to bottom, v= 1.5, 1.4, 1.3, and 1.2. (b) The solid line is vertical velocity corresponding to the long-wavelength minimum with v=1.3. The short-dashed line is vertical velocity corresponding to the short-wavelength minimum with v=1.4. The dotted line is temperature perturbation of the long-wavelength solution. The long-dashed line is temperature perturbation of the short-wavelength solution.

It must be noted, however, that when a phase transition and a converging background flow are present, the dynamics are very sensitive to the exact values of the parameters and to the width and shape of the boundary layer. It was found that for v=1.3 a Clapeyron slope of -2 MPa/K is unstable at negative Rayleigh numbers, while a value of -3.2MPa/K shows only completely layered solutions with Rayleigh numbers of 328. Small variations in the background velocity show similar sensitivity as do variations in the boundary layer thickness and shape, and we have no method of determining an appropriate velocity convergence for a particular value of the system Rayleigh number. However, given the similarity between the nonlinear model results and those found here, it seems likely that the Earth, or at least the nonlinear models of the Earth that have been explored numerically, is (are) operating in a region of parameter space in which the Clapeyron slope is subcritical but the minimum critical Rayleigh number for the avalanche solution is positive. There are then seen to be two ways of "triggering" an avalanche. Either the background velocity convergence decreases, decreasing the critical Rayleigh number required to cause the instability, or the boundary layer Rayleigh number increases owing to an increase in the temperature contrast or to an increase in boundary layer thickness. Once a boundary layer is destroyed, flow across the phase transition once more becomes inhibited and it takes time for the boundary layer to be built up to a critical state again by the background flow, resulting in the quasi-periodicity (intermittency) observed in the simulations.

Calculations in spherical coordinates have also been performed with a phase transition and background convergence, and in all cases the results were very similar to the results obtained for the calculations performed in Cartesian geometry. Figure 11b shows the analogous neutral curves to those in Figure 11a for the sphere. We see that they are qualitatively extremely similar. Of course, in the spherical case the wavelength spectrum is discrete and thus results are shown only for the wavelength corresponding to discrete values of spherical harmonic degree. One small difference is that the instability in the spherical case becomes layered for slightly less negative values of the Clapeyron slope. In Figure 11b the critical Clapeyron slope is seen to be between -2.54 and -2.55 MPa/K.

Discussion and Conclusions

Thermal boundary layers in the absence of the influence of phase transitions and dynamical effects were shown to be highly unstable when situated in a deep layer. Boundary layers situated at the center of deep

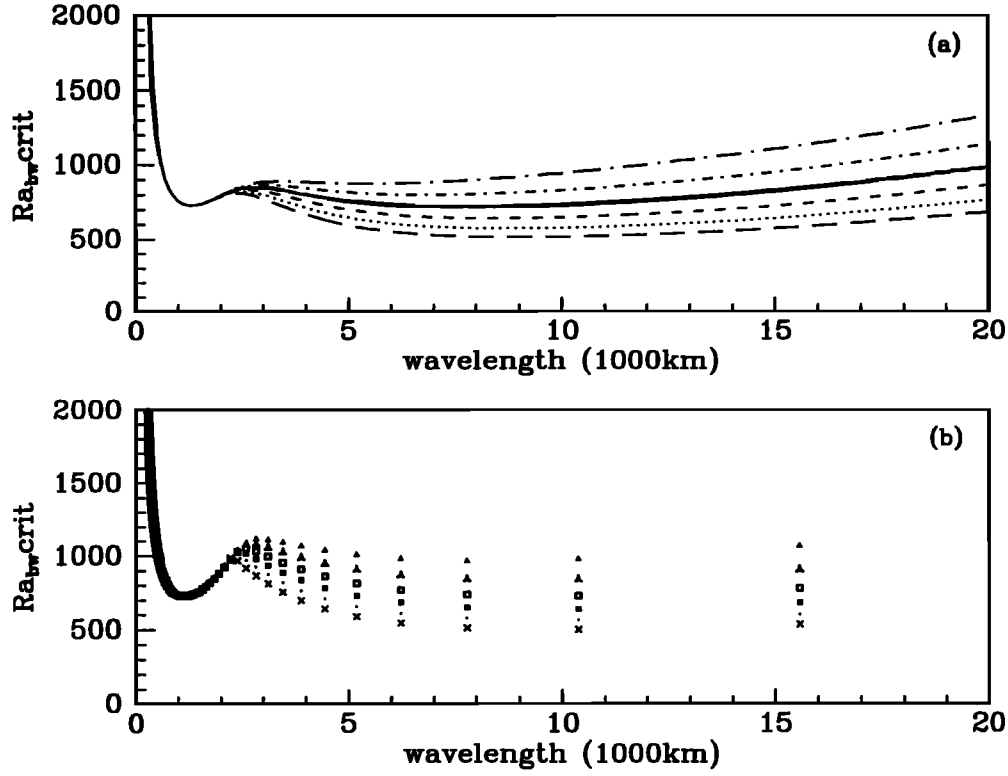

Figure 11. (a) Neutral curves with v=1.4 with varying Clapeyron slopes in Cartesian coordinates and $DT = -2.25\text{sech}^2[4.5(z - z_0)]$, showing the change from an avalanche type instability to the layered mode for decreasing values of the endothermic Clapeyron slope. The Clapeyron slope corresponding to the curve represented by the long-dashed line is γ=-2.55 MPa/K, for the dotted line is γ=-2.56 MPa/K, for the short-dashed line is γ=-2.57 MPa/K, for the solid line is γ= -2.58 MPa/K, for the short-dash-dotted line is γ=-2.59 MPa/K, and for the long-dash-dotted line is γ=-2.6 MPa/K. (b)Neutral curves with v=1.4 for varying values of the Clapeyron slope in spherical coordinates and $DT = -2.25\text{sech}^2[4.5(r - r_0)]$. The Clapeyron slopes corresponding to the curve marked by the crosses, dots, solid squares, open squares, stars and triangles are -2.51, -2.52, -2.53, -2.54, -2.55, and -2.56 MPa/K, respectively.

fluid regions were shown to be particularly unstable, and stability increased as the region of strong vertical temperature gradient was moved closer to an impermeable boundary. The length scales controlling the dynamics were shown to be the entire layer depth and the distance to the closest impermeable boundary. The depth of the thermal boundary layer was shown to exert very little influence on the dynamics as long as it was shallower than one tenth of the full layer depth. In this case the thermal boundary layer was shown to be well approximated by a delta function temperature gradient at the appropriate depth. As a result, the spatial extent of convection at the critical Rayleigh number arising from thermal boundary layers is not limited to the region of the boundary layer but, rather, it fills the entire fluid layer in which the boundary layer is contained. This result is consistent with the divergence of the correlation length of a convective cell at the critical Rayleigh number [e.g., *Zaitsev and Shliomis*, 1971].

In the absence of background flow and phase transitions the thermal boundary layer at 660 km that was shown to develop in the simulations of *Solheim and Peltier* [1994a, b] was observed to be unstable at extremely small Rayleigh numbers, but the instability that ensued was consistent with the spatial extent of an avalanche. The presence of the endothermic phase transition alone at 660 km depth was seen to further destabilize the layer, and this was shown to be a result of the fact that endothermic phase transitions are increasingly destabilizing the deeper the layer of fluid in which they exist, in accord with arguments of *Peltier* [1985].

A criterion for determining whether a Rayleigh-Taylor instability will be avalanche-like or layered was discussed, and this was shown to depend critically on the boundary layer thickness. In the considerably more complex thermal instability this criterion was shown to offer insight into the importance of boundary layer thickness and velocity convergence in determining the stability of the boundary layer.

A converging flow was seen to stabilize a thermal boundary layer, possibly explaining the region of stability of the thermal boundary layers observed in high Rayleigh number numerical simulations of the convection process. The values of the velocity convergence required to achieve critical boundary layer Rayleigh num-

bers comparable to those in the simulation of *Solheim and Peltier* [1994a] were unrealistically high in the absence of the influence of the endothermic phase transition itself. When coupled with the influence of the endothermic phase transition, however, the applied velocity convergence was shown to be very strongly stabilizing. Stabilization increased with decreasing Clapeyron slope and increasing velocity convergence. A critical Clapeyron slope for a given value of the velocity convergence was shown to exist, below which, only layered convection solutions exist, and above which, avalanche solutions occurred. The effects of sphericity were shown not to affect these results significantly. The results obtained through application of linear stability analysis to an internal thermal boundary layer in the Earth-like geometry and an assessment of the extent of the agreement of these results with the simulations of Solheim and Peltier are summarized in Table 2. This stabilization of a thermal boundary layer by a uniform strain field is quite similar to the stabilization of a vorticity strip against Kelvin- Helmholtz instability by a strain field [e.g., *Dritchel et al.,* 1991] in infinite Reynolds number flow.

A number of potentially important effects have not been dealt with in the analysis reported herein, however. The influence of internal heating, in particular, has not been considered, although it is likely that this will simply accentuate the downwellings from the upper surface, increasing the convergence onto the boundary layer and hence should be stabilizing, as has already been demonstrated to be the case in the numerical simulations of *Solheim and Peltier* [1994a]. Also, non-Boussinesq effects have been neglected. Although these will probably affect the results quantitatively, it is quite clear that in their presence a converging flow onto an endothermic phase transition will still be stabilizing. Effects due to variations in viscosity, thermal conductivity, and the thermodynamic coefficients have also been neglected. It remains to be seen whether these will influence the ability of velocity convergence to stabilize the boundary layer. Also, the Clapeyron slope of the 660-km phase transition is only constrained to lie within the range -2 to -6 MPa/K according to *Ito and Takahashi* [1989], although *Chopelas et al.* [1994] found it to be more strongly constrained to a value near -3 MPa/K. Although our model is quite sensitive to the exact value of the Clapeyron slope, it has been shown that for any value of the Clapeyron slope there is a velocity convergence for which the avalanche solution obtains at the minimum Rayleigh number and where if the velocity convergence is sufficiently high, layered convection will be the only possible form. Clearly, a constant velocity convergence is an enormous simplification of the influence of the real, time dependent, background

Table 2. Effects Included in the Analysis of Convective Instability for Earth-Like Geometry and Comparison with the Numerical Experiments of *Solheim and Peltier* [1994a, b]

Included Effects	Type of Case	Agreement With Numerical Experiment	Disagreement with Numerical Experiment
1	pure thermal convective	velocity eigenfunction structure is compatible with observed avalanches	Ra_{min} is many orders of magnitude smaller than those obtained in the numerical experiments, no layered solutions are found, the boundary layer width is found not to play a significant role in the instability
2	Rayleigh-Taylor limit with phase transition	avalanche solutions and layered solutions are observed, layering increases with decreasing Clapeyron slope and decreasing boundary layer width	timescale for instability is 2 orders of magnitude too short, no stable regime exists
1,2	thermal case with phase transition	avalanche solutions are seen	Ra_{min} is negative; no layering is observed
1,3	thermal case with velocity convergence	avalanche solutions are seen; Ra_{min} is higher than in the absence of velocity convergence	Ra_{min} is similar to values observed in the numerical experiments only if an unrealistically large velocity convergence is used, no layered solutions are observed
1,2,3	thermal case with phase transition and velocity convergence	avalanches and layered regimes are observed; layering increases with decreased boundary layer width, with decreasing Claperon slope, and increased velocity convergence	

Included physical effects are denoted by the following numbering scheme: 1, thermal conductivity; 2, endothermic phase transition at 660 km depth; 3, velocity convergence.

flow; horizontal and vertical variations in vertical velocity have been neglected, while horizontal velocity has been neglected entirely. Also, continuity is not satisfied at the phase boundary or at the outer boundaries. The Péclet number parametrization is intended, however, to capture only the effect of the heat advection convergence, and it is the intention of our calculation to represent this in the simplest possible fashion in order to gain physical insight into the avalanche process. Since this simple parameterization appears to explain many of the features seen in the full nonlinear simulations, it would appear that we have effectively captured much of the important physics governing the avalanche process. It is intended to further test the hypothesis developed herein, that it is velocity convergence onto the boundary layer and its interaction with the phase transition that stabilizes the thermal boundary layer in the above cited numerical simulations, using a series of especially designed nonlinear simulations. Such further analyses will be reported in due course.

References

Bercovici, D., G. Schubert, and P.J. Tackley, On the penetration of the 660 km phase change by mantle downflows, *Geophys. Res. Lett., 20,* 2599-2602, 1993.

Buffet, B., C. Gable, and R. O'Connell, Linear stability of a layered fluid with mobile surface plates, *J. Geophys. Res., 99,* 19,885-19,900, 1994.

Busse, F., and G. Schubert, Convection in a fluid with two phases, *J. Fluid. Mech., 46,* 801-812, 1971.

Chandrasekhar, S., *Hydrodynamic and Hydromagnetic Stability,* Dover, 652 pp., N. Y., 1961.

Chopelas, A., R. Boehler, and T. Ko, Thermodynamics and behaviour of Mg_2SiO_4 at high pressure: Implications for $\gamma - Mg_2SiO_4$ phase equilibrium, *Phys. Chem. Miner., 21,* 351-359, 1994.

Davies G., Punctuated tectonic evolution of the earth, *Earth Planet. Sci. Lett., 136,* 363-379, 1995.

Dritchel, D., P. Haynes, M. Juckes, and T.G. Shepherd, The stability of a two-dimensional vorticity filament under uniform strain, *J. Fluid Mech., 230,* 647-665, 1991.

Honda, S., D.A. Yuen, S. Balachandar, and D. Reuteler, Three-dimensional instabilities of mantle convection with multiple phase transitions, *Science, 259,* 1308-1311, 1993.

Howard, L.N., Convection at high Rayleigh number, in *Proceedings of the XI International Congress of Applied Mechanics, Munich, 1964,* edited by H.Goertler, pp. 1109-1115, Springer-Verlag, Berlin, 1966.

Ito, E., and E. Takahashi, Postspinel transformations in the system Mg_2Si_4-$FeSiO_4$ and some geophysical implications, *J. Geophys. Res., 94,* 10,637-10,646, 1989.

Jarvis, T., and W.R. Peltier, Mantle convection as a boundary layer phenomenon, *Geophys. J. R. Astron. Soc., 68,* 389-427, 1982.

Machetel, P., and P. Weber, Intermittent layered convection in a model mantle with an endothermic phase change at 670 km, *Nature, 350,* 55-57, 1991.

Peltier, W.R., Penetrative convection in the planetary mantle, *Geophys. Fluid Dyn., 5,* 47-88, 1972.

Peltier, W.R., Mantle convection and viscoelasticity, *Annu. Rev. Fluid Mech., 17,* 561-608, 1985.

Peltier, W.R., Phase-transition modulated mixing in the mantle of the Earth, *Philos. Trans. Roy. Soc. London, Ser. A, 354,* 1425-1447, 1996.

Peltier, W.R.,and L.P. Solheim, Mantle phase transitions and layered chaotic convection, *Geophys. Res. Lett., 19,* 321-324, 1992.

Peltier, W.R., S. Butler, and L.P. Solheim, The influence of phase transformations on mantle mixing and plate tectonics, in *The Earth's Deep Interior,* edited by D. Crossley, pp. 405-430, Gordon and Breach, Newark N.J., 1996.

Schubert, G., and D.L. Turcotte, Phase changes and mantle convection, *J. Geophys. Res., 76,* 1424-1432, 1971.

Sharpe, H., and W.R. Peltier, A thermal history model for the earth with parameterized convection, *Geophys. J. R. Astron. Soc., 59,* 171-203, 1979.

Solheim, L.P., and W.R. Peltier, Avalanche effects in phase transition modulated thermal convection: A model of the Earth's mantle, *J. Geophys. Res., 99,* 6997-7018, 1994a.

Solheim, L.P., and W.R. Peltier, Phase boundary deflections at 660-km depth and episodically layered isochemical convection in the mantle, *J. Geophys. Res., 99,* 15,861-15,875, 1994b.

Tackley, P.J., On the penetration of an endothermic phase transition by upwellings and downwellings, *J. Geophys. Res., 100,* 15,477-15,488, 1995.

Tackley, P.J., D.J. Stevenson, G.A. Glatzmaier, and G. Schubert, Effects of an endothermic phase transition at 670 km depth in a spherical model of convection in the Earth's mantle, *Nature,* 361, 699-704, 1993.

Tackley, P.J., D.J. Stevenson, G.A. Glatzmaier, and G. Schubert, Effects of multiple phase transitions in a three-dimensional spherical model of convection in Earth's mantle, *J. Geophys. Res., 99,* 15,877-15,901, 1994.

Yuen, D., W.R. Peltier, and G. Schubert, On the existence of a second scale of convection in the upper mantle, *Geophys. J. R. Astron. Soc., 65,* 171-190, 1981.

Zaitsev, V., and M. Shliomis, Hydrodynamic fluctuations near the convection threshold, *Sov. Phys. JETP,* Engl. Transl., *32,* 866-870, 1971.

S. Butler and W. R. Peltier, Department of Physics, University of Toronto, 60 St. George Street, Toronto, Ontario, Canada M5S 1A7. (email: sam@atmosp.physics.utoronto.ca; peltier@atmosp.physics.utoronto.ca)

(Received April 10, 1996; revised September 30, 1996; accepted October 14, 1996.)